ChemComm

COMMUNICATION

View Article Online
View Journal | View Issue

Check for updates

Cite this: *Chem. Commun.*, 2020, **56**, 14829

Received 14th August 2020,
Accepted 30th October 2020

DOI: 10.1039/d0cc05539e

rsc.li/chemcomm

Published on 02 November 2020. Downloaded on 2/14/2026 6:06:56 AM.

S-Mg_2(dobpdc): a metal–organic framework for determining chirality in amino acids†

Hui Min Tay, [a] Aditya Rawal[b] and Carol Hua *[a]

Chirality is a key aspect of amino acids and is essential for life. Here, a chiral metal–organic framework, *S*-Mg_2dobpdc, is used to determine the chirality of three BOC protected amino acids (alanine, valine and proline) by ^{13}C solid-state NMR with chemical shift differences of up to 1.3 ppm observed between enantiomers. The chiral sensitivity persists upon *in situ* deprotection of the amino acids by thermolysis of the BOC group.

Amino acids are the building blocks of proteins and an important component in chemical and biological systems. The different enantiomers of amino acids can lead to vastly different physiological and metabolic outcomes. The growing use of amino acid derivatives in pharmacology, chemical science and biochemistry highlights the need for efficient methods to determine chiral purity. The elucidation of chirality in amino acids can be challenging due to their lack of strong chromophoric groups, leading to a weak chiro-optical response in circular dichroism spectroscopy,[1] or the need for multiple protection, derivation and deprotection steps. The majority of chiral elucidation methods involve the use of chromatographic techniques, including HPLC and GC,[2] or optical methods, including fluorescence and luminescence.[3] Solid-state NMR offers a direct means of identifying and quantifying the enantiopurity of a sample. The use of solid-state NMR for the quantification of chirality is underdeveloped, with the main focus in this area concerning the use of liquid crystals as a chiral matrix.[8,9]

Coordination Polymers (CPs) and Metal Organic Frameworks (MOFs) are crystalline solid materials comprising of metal ions bridged by organic ligands in 1D, 2D or 3D to create a scaffold containing pores.[4] Chiral MOFs and CPs are typically used as stationary chiral phases for HPLC[5] or as heterogenous asymmetric catalysts.[6] Considerably less attention has been focussed on the use of MOFs and CPs for the detection of chiral purity. Developments in this area with MOFs and CPs primarily utilise optical spectroscopic techniques, including fluorescence and UV-Vis.[7] CPs and MOFs can potentially act as solid-state chiral solvating agents due to their tunable pores, which can form strong intermolecular interactions with chiral guests, resulting in a diastereomeric complex observable by NMR. While solid-state NMR spectra can have large peak widths, making the small chemical shifts between diastereomers difficult to resolve, MOFs and CPs are crystalline materials that typically have narrow peak widths and sharp NMR resonances.

While three previous reports have used MOFs for chiral elucidation, none of these were able to differentiate between enantiomers from a racemic mixture.[10–12] Only small chemical shift differences of up to 0.4 ppm were observed in the ^{13}C NMR spectra of a chiral analogue of the UMCM-1 framework[11] upon loading with enantiopure 1-phenyl-2,2,2-trifluoroethanol (TFPE), or when alanine and leucine were loaded into $[Zn_2(\text{L-Phe})(\text{bpe})_2]_n$ (L-Phe = L-phenylalanine, bpe = bis(4-pyridyl)ethylene).[12]

Long *et al.* recently reported the synthesis of a chiral form of Mg_2dobpdc (H_4dobpdc = 4,4′-dioxidobiphenyl-3,3′-dicarboxylic acid).[13] The axial chirality of Mg_2dobpdc results from the rotation of the two phenyl rings in dobpdc^{4-} relative to each other, yielding enantiomerically pure domains of solely right-handed or left-handed helices. The grafting of chiral 1,2-diaminocyclohexane enabled the solid-state NMR characterisation of the ammonium carbamate chains formed upon the adsorption of CO_2 to yield chemical shift differences of up to 2.0 ppm. Mg_2(dobpdc) (and its Zn^{II} analogue) have been extensively studied by solid-state NMR,[14–19] including in experiments that probe molecular dynamics using ^{15}N NMR[20] and investigations of local disorder by ^{25}Mg NMR.[21,22] The breadth of information concerning the behaviour of Mg_2(dobpdc) makes it a valuable target for the study of chiral elucidation by solid-state NMR.

Herein, we present the use of *S*-Mg_2dobpdc for the chiral elucidation of amino acids using ^{13}C solid-state NMR. *S*-Mg_2dobpdc

[a] *School of Chemistry, The University of Melbourne, Parkville, Victoria, 3010, Australia. E-mail: carol.hua@unimelb.edu.au*
[b] *Mark Wainwright Analytical Centre, University of New South Wales, Kensington, New South Wales, 2052, Australia*

† Electronic supplementary information (ESI) available: Thermal gravimetric analysis (TGA) traces, powder X-ray diffraction (PXRD) patterns, ATR infrared spectra (IR), solution state NMR spectra and additional ^{13}C CPMAS spectra. See DOI: 10.1039/d0cc05539e

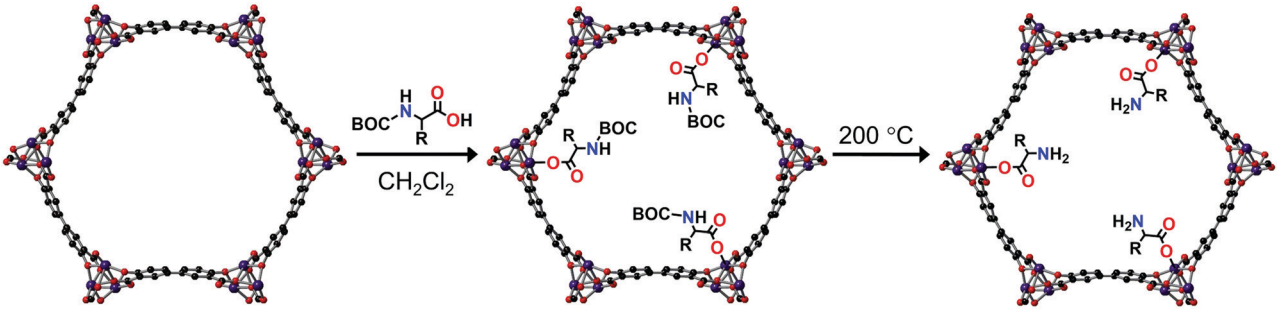

Fig. 1 Schematic of the appendage of BOC protected amino acids to the open Mg^{II} metal sites on *S*-Mg_2dobpdc to yield *S*-Mg_2dobpdc@BOC-Xxx (Xxx = Ala, Val, Pro) where R = CH_3 (alanine), ^{i}Pr (valine), $CHCH_2CH_2CH_2$ (proline) followed by the thermal deprotection of the BOC group to yield *S*-Mg_2dobpdc@Xxx (Xxx = Ala, Val, Pro). The appendage of amino acids to 50% of Mg^{II} metal sites is shown here for clarity. The atoms are represented as follows: magnesium (purple), carbon (black), oxygen (red).

Published on 02 November 2020. Downloaded on 2/14/2026 6:06:56 AM.

was grafted post-synthetically with enantiopure BOC alanine, valine and proline to the Mg^{II} metal site. Unprotected amino acids were obtained by thermal deprotection of the BOC groups post-grafting. The ^{13}C NMR chemical shift differences between the L- and D-enantiomers of the BOC protected and free amino acids as well as the *S*-Mg_2dobpdc framework were determined and the mode of binding discussed.

S-Mg_2(dobpdc) was made according to the procedure reported by Long *et al.*[13] Enantiomerically pure di-*tert*-butyl dicarbonate (BOC) protected alanine, valine and proline were then grafted onto the framework to yield *S*-Mg_2(dobpdc)@BOC-L-Xxx (Xxx = Ala, Val, Pro) and *S*-Mg_2(dobpdc)@BOC-D-Xxx (Xxx = Ala, Val, Pro), as white powders (Fig. 1). The BOC group ensured that coordination to the Mg^{II} metal centre only occurred through the carboxylic acid instead of the primary amine of the amino acid. Alanine, valine and proline were chosen for incorporation to minimise the steric bulk present, ensuring that a high percentage loading and strong intermolecular interactions to the framework could be achieved. Amino acids with aliphatic side chains enabled easy identification from the aromatic dobpdc^{4-} ligand in NMR studies. The PXRD of *S*-Mg_2(dobpdc)@BOC-Xxx (Xxx = Ala, Val, Pro) verified that the crystallinity and structure of the *S*-Mg_2(dobpdc) framework had been retained (ESI,† Fig. S1–S4). The incorporation of the BOC amino acid guest into *S*-Mg_2dobpdc was verified by the BOC carbonyl peak in the FT-IR spectrum at 1670 cm^{-1} (ESI,† Fig. S5–S7) and *via* solution-state ^{1}H NMR spectroscopy of the digested samples of *S*-Mg_2(dobpdc)@BOC-Xxx (Xxx = Ala, Val, Pro) (ESI,† Fig. S8–S13).

The thermal gravimetric analyses (TGA) of *S*-Mg_2(dobpdc)@BOC-Xxx (Xxx = Ala, Val, Pro) displayed three stepwise mass losses (ESI,† Fig. S14–S22). The first mass loss below 100 °C was attributed to the loss of water adsorbed from the atmosphere. The second mass loss between 100 and 200 °C was due to the thermal deprotection of the BOC group from the appended BOC amino acids. The post-synthetic deprotection of the BOC group from proline within a MOF has previously been reported.[23–25] The third mass loss between 220 and 280 °C is due to thermal decomposition of the amino acids into gaseous products and can be correlated to the size of the side chain, with *S*-Mg_2(dobpdc)@BOC-Val having the largest mass loss.[26,27]

The thermal BOC deprotection of the amino acids was confirmed by FT-IR measurements after heating the *S*-Mg_2(dobpdc)@BOC-Xxx (Xxx = Ala, Val, Pro) samples at 200 °C for 30 mins to yield *S*-Mg_2(dobpdc)@Xxx, where the BOC carbonyl peak at 1670 cm^{-1} disappeared (ESI,† Fig. S23–S25). The conversion of BOC-Ala to Ala resulted in red shifts of the FT-IR absorption bands to wavelengths similar to those for the Mg_2dobpdc framework. Remarkably, PXRD measurements (ESI,† Fig. S26–S28) confirmed that crystallinity was retained after BOC deprotection. In the TGA of *S*-Mg_2(dobpdc)@Xxx (Xxx = Ala, Val, Pro), the mass loss between 100 and 200 °C was absent, confirming the successful deprotection of the BOC group (ESI,† Fig. S29–S31).

As the removal of the BOC group can be directly observed from the mass loss in the TGA traces, this was used to determine the percentage incorporation of the amino acid, which was verified by elemental analysis. The highest percentage loading was achieved with BOC-Ala (57%), followed by BOC-Pro (55%) and BOC-Val (39%). It is likely that both the degree of steric bulk and the conformation of the amino acid had an effect on the amount of amino acid incorporated into *S*-Mg_2(dobpdc). DMF solvent molecules remained coordinated to the Mg^{II} metal sites that have no amino acid appended, even after heating the samples at 200 °C, as observed in the ^{13}C CPMAS spectra (*vide infra*).

The *S*-Mg_2dobpdc framework and the amino acid appended samples were analysed by ^{13}C solid-state NMR (Fig. 2). The ^{13}C CPMAS spectrum of *S*-Mg_2dobpdc contained well-defined spectral lines with widths at half height of 0.7 ppm, enabling all the ^{13}C resonances arising from the dobpdc^{4-} ligand to be assigned (ESI,† Fig. S33). A ^{13}C non-quaternary suppression (NQS) experiment was used to assign the quaternary carbon resonances (ESI,† Fig. S34–S36).

The ^{13}C CPMAS spectra of *S*-Mg_2(dobpdc)@BOC-Xxx (Xxx = Ala, Val, Pro) showed distinct chemical shift differences of up to 0.6 ppm in specific ^{13}C NMR resonances between the L- and D-amino acids (Fig. 2a–c and Fig. S37–S42, ESI†). The largest chemical shift occurred at **C2**, **C3**, **C4**, **C5** and $\mathbf{C_e}$, suggesting that the methyl groups from the BOC group are involved in CH–π intermolecular interactions with the phenyl

 This journal is © The Royal Society of Chemistry 2020

Published on 02 November 2020. Downloaded on 2/14/2026 6:06:56 AM.

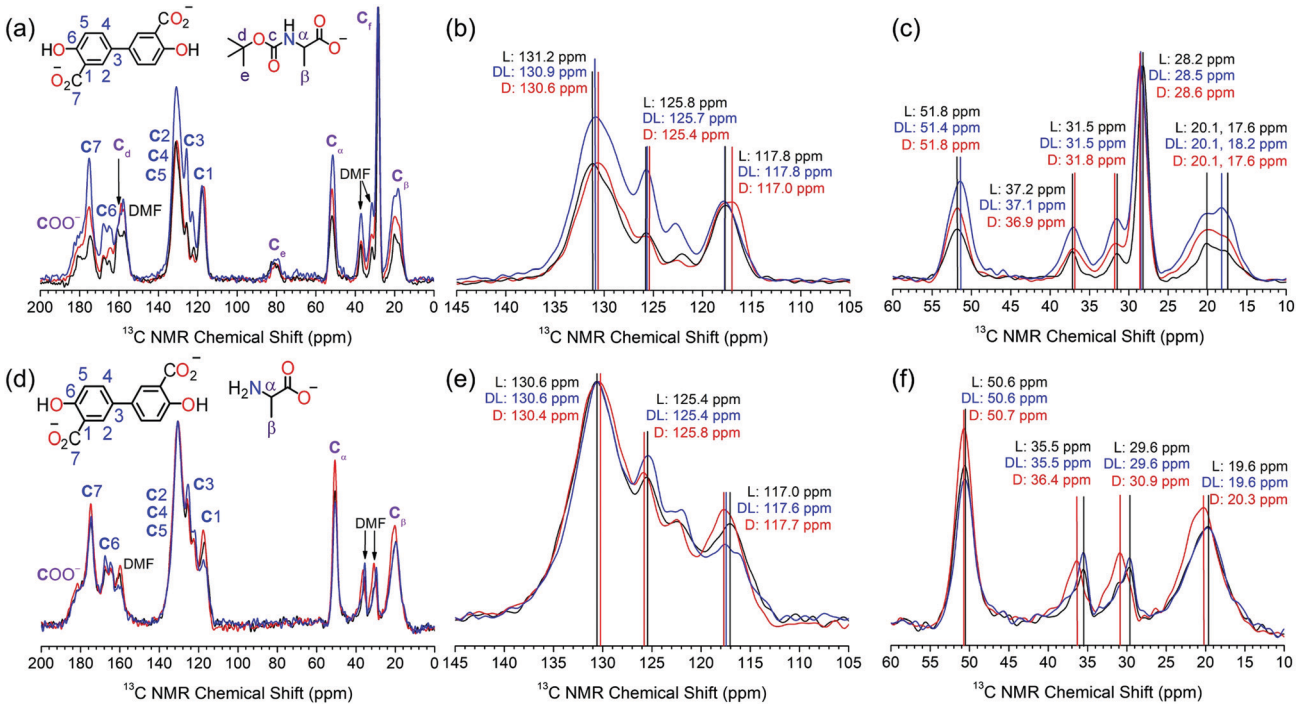

Fig. 2 ^{13}C solid state CPMAS spectra of Mg_2dobpdc@BOC-L-Ala (black), Mg_2dobpdc@BOC-D-Ala (red) and Mg_2dobpdc@BOC-DL-Ala (blue) acquired at 175 MHz showing (a) the full spectrum between 200–0 ppm, (b) zoomed in section between 145–105 ppm, and (c) zoomed in section between 60–10 ppm. The ^{13}C solid state CPMAS spectra of Mg_2dobpdc@L-Ala (black), Mg_2dobpdc@D-Ala (red) and Mg_2dobpdc@DL-Ala (blue) acquired at 175 MHz showing (d) the full spectrum between 200–0 ppm, (e) zoomed in section between 145–105 ppm, and (f) zoomed in section between 45–10 ppm. All spectra are scaled to the same maximum intensity.

rings of the dobpdc^{4-} ligand. Remarkably, the **C2–C5** signals of dobpdc^{4-} can be used to discriminate between the L and D enantiomers of BOC-Ala by the ^{13}C NMR chemical shift. Mg_2dobpdc@BOC-DL-Ala (comprised of 60% BOC-L-Ala, 40% BOC-D-Ala) has a chemical shift of 130.9 ppm, which is intermediate between that of Mg_2dobpdc@BOC-L-Ala (131.2 ppm) and Mg_2dobpdc@BOC-D-Ala (130.6 ppm) (Fig. 2b). ^{13}C chemical shift differences also occur for **C3** and $\mathbf{C_\beta}$. It is surprising that no changes in the chemical shift were observed for $\mathbf{C_\alpha}$, given this is where the stereocentre is located, however, chiral elucidation in *S*-Mg_2dobpdc likely involves the different orientations of the amino acid relative to the aromatic rings of dobpdc^{4-}. A similar interaction was observed for UMCM where the ^{13}C resonances of the framework, instead of the stereocentre, changed upon the incorporation of chiral guest molecules.[11]

The largest chemical shift changes were observed for alanine, followed by proline (ESI,† Fig. S37–S39), then valine (ESI,† Fig. S40–S42). This trend is attributed to the size of the amino acid side chain, with the small methyl side chain in alanine enabling the amino acid to effectively interact with *S*-Mg_2dobpdc. The valine isopropyl side chain has greater steric bulk, precluding the formation of strong intermolecular interactions required for effective chiral discrimination. The orientation of the side chain relative to the carboxylate and BOC groups of the amino acid is also an important consideration. The restricted movement of the five membered pyrrolidene ring in proline likely helps to yield a geometry that allows enhanced interaction with the dobpdc^{4-} ligand.

The steric effect of the BOC group on chiral discrimination by ^{13}C solid state NMR was additionally investigated by analysis of the deprotected amino acid samples of *S*-Mg_2dobpdc@Ala. The ^{13}C CPMAS spectra of *S*-Mg_2(dobpdc)@L-Ala and *S*-Mg_2(dobpdc)@D-Ala displayed enhanced ^{13}C chemical shift differences of up to 1.3 ppm when compared with the BOC-protected samples, with the largest chemical shift differences observed for the CH_3 groups of DMF, followed by that of **C1** and $\mathbf{C_\beta}$ (Fig. 2d–f). The removal of the bulky BOC group enables a stronger interaction between the amino acid and the framework components, thereby enhancing chiral elucidation. The broad $\mathbf{C_\beta}$ peak of alanine becomes narrower when the BOC group is removed, indicating that the BOC group may cause some conformational disorder. When the framework was loaded with DL-Ala, the ^{13}C chemical shifts more closely resembled that of Mg_2(dobpdc)@L-Ala than Mg_2(dobpdc)@D-Ala. This is consistent with the composition of DL-Ala, which consists of a 60 : 40 ratio of L- to D-Ala.

The linewidths in the NMR spectra of the amino acid loaded frameworks were broader than for *S*-Mg_2(dobpdc), with linewidths at half height of 1.8 ppm. This can be attributed to the local disorder of the Mg^{II} environment upon guest loading. Previous studies of ^{25}Mg NMR on *rac*-Mg_2dobpdc and Mg_2dobdc (dobdc^{4-} = 2,5-dihydroxyterephthalate) have shown that although long-range ordering is maintained upon dehydration and guest loading, slight changes in the orientation of the ligands result in small changes in the Mg–O bond length and O–Mg–O bond angle to yield local disorder.[21,22]

Published on 02 November 2020. Downloaded on 2/14/2026 6:06:56 AM.

The porous and robust *S*-Mg_2dobpdc framework was shown to be highly effective for chiral elucidation by ^{13}C solid state NMR with BOC-alanine, BOC-valine, BOC-proline and alanine with up to a 1.3 ppm difference. The chemical shift changes between the L- and D-amino acids were attributed to intermolecular interactions between the amino acid and the aromatic protons of *S*-Mg_2dobpdc. The largest changes in the ^{13}C chemical shift between the L- and D-enantiomers occur in alanine-loaded frameworks due to the low steric bulk of the side chain which enables strong intermolecular interactions to be formed with *S*-Mg_2dobpdc. It is noted that *S*-Mg_2dobpdc is locally sensitive to the chirality of the amino acid which is detected by ^{13}C NMR, but is unable to be detected by PXRD, which measures long range ordering. Future studies include the analysis of other amino acids, including those containing aromatic side chains and additional Hydrogen bonding sites, as well as computational calculations to determine the origin of the ^{13}C chemical shift difference between enantiomers. This study has demonstrated that solid-state NMR spectroscopy together with chiral MOFs is a versatile and elegant approach to overcoming the challenges of chiral elucidation for amino acids.

We thank Dr Doug Lawes for assistance with ^1H solution state NMR, Dr Marc-Antione Sani for preliminary solid-state NMR experiments, Ms Lisa Hua for experimental assistance and A/Prof. Brendan Abrahams for support during this work. H. M. T. thanks the Australian Commonwealth Government and the University of Melbourne for a Research Training Programme Scholarship, Rowden White Scholarship and an Elizabeth and Vernon Puzey Scholarship. C. H. gratefully acknowledges the University of Melbourne for a McKenzie Fellowship.

Conflicts of interest

There are no conflicts to declare.

Notes and references

1 C. Wolf and K. W. Bentley, *Chem. Soc. Rev.*, 2013, **42**, 5408–5424.
2 M. Dołowy and A. Pyka, *Biomed. Chromatogr.*, 2014, **28**, 84–101.
3 J. Wang, H.-B. Liu, Z. Tong and C. S. Ha, *Coord. Chem. Rev.*, 2015, **303**, 139–184.
4 H. Furukawa, K. E. Cordova, M. O'Keeffe and O. M. Yaghi, *Science*, 2013, **341**, 1230444.
5 T. Duerinck and J. F. M. Denayer, *Chem. Eng. Sci.*, 2015, **124**, 179–187.
6 C. Wang, M. Zheng and W. Lin, *J. Phys. Chem. Lett.*, 2011, **2**, 1701–1709.
7 X. Zhang, J. Yin and J. Yoon, *Chem. Rev.*, 2014, **114**, 4918–4959.
8 T. J. Wenzel, *Discrimination of Chiral Compounds Using NMR Spectroscopy*, John Wiley & Sons, Hoboken, New Jersey, 2007.
9 A. Kumar and N. Suryaprakash, *Two-Dimensional NMR of Molecules Oriented in Liquid Crystals-Recent Developments*, John Wiley & Sons, Ltd, 2007.
10 C. Kutzscher, H. C. Hoffmann, S. Krause, U. Stoeck, I. Senkovska, E. Brunner and S. Kaskel, *Inorg. Chem.*, 2015, **54**, 1003–1009.
11 H. C. Hoffmann, S. Paasch, P. Müller, I. Senkovska, M. Padmanaban, F. Glorius, S. Kaskel and E. Brunner, *Chem. Commun.*, 2012, **48**, 10484–10486.
12 X. Ma, Y. Zhang, Y. Gao, X. Li, C. Wang, H. Yuan, A. Yu, S. Zhang and Y. Cui, *Chem. Commun.*, 2020, **56**, 1034–1037.
13 J. D. Martell, L. B. Porter-Zasada, A. C. Forse, R. L. Siegelman, M. I. Gonzalez, J. Oktawiec, T. Runčevski, J. Xu, M. Srebro-Hooper, P. J. Milner, K. A. Colwell, J. Autschbach, J. A. Reimer and J. R. Long, *J. Am. Chem. Soc.*, 2017, **139**, 16000–16012.
14 A. C. Forse, S. A. Altobelli, S. Benders, M. S. Conradi and J. A. Reimer, *J. Phys. Chem. C*, 2018, **122**, 15344–15351.
15 A. C. Forse, M. I. Gonzalez, R. L. Siegelman, V. J. Witherspoon, S. Jawahery, R. Mercado, P. J. Milner, J. D. Martell, B. Smit, B. Blümich, J. R. Long and J. A. Reimer, *J. Am. Chem. Soc.*, 2018, **140**, 1663–1673.
16 A. C. Forse, K. A. Colwell, M. I. Gonzalez, S. Benders, R. M. Torres-Gavosto, B. Blümich, J. A. Reimer and J. R. Long, *Chem. Mater.*, 2020, **32**, 3570–3576.
17 P. J. Milner, R. L. Siegelman, A. C. Forse, M. I. Gonzalez, T. Runčevski, J. D. Martell, J. A. Reimer and J. R. Long, *J. Am. Chem. Soc.*, 2017, **139**, 13541–13553.
18 A. C. Forse, P. J. Milner, J. H. Lee, H. N. Redfearn, J. Oktawiec, R. L. Siegelman, J. D. Martell, B. Dinakar, L. B. Porter-Zasada, M. I. Gonzalez, J. B. Neaton, J. R. Long and J. A. Reimer, *J. Am. Chem. Soc.*, 2018, **140**, 18016–18031.
19 R. L. Siegelman, P. J. Milner, A. C. Forse, J. H. Lee, K. A. Colwell, J. B. Neaton, J. A. Reimer, S. C. Weston and J. R. Long, *J. Am. Chem. Soc.*, 2019, **141**, 13171–13186.
20 J. Xu, Y. M. Liu, A. S. Lipton, J. Ye, G. L. Hoatson, P. J. Milner, T. M. McDonald, R. L. Siegelman, A. C. Forse, B. Smit, J. R. Long and J. A. Reimer, *J. Phys. Chem. Lett.*, 2019, **10**, 7044–7049.
21 J. Xu, V. V. Terskikh and Y. Huang, *J. Phys. Chem. Lett.*, 2013, **4**, 7–11.
22 J. Xu, E. S. M. Blaakmeer, A. S. Lipton, T. M. McDonald, Y. M. Liu, B. Smit, J. R. Long, A. P. M. Kentgens and J. A. Reimer, *J. Phys. Chem. C*, 2017, **121**, 19938–19945.
23 X. Zhou, F. Xu, Z. Wu, H. Li and S. Yang, *ACS Omega*, 2019, **4**, 8588–8597.
24 C. Kutzscher, G. Nickerl, I. Senkovska, V. Bon and S. Kaskel, *Chem. Mater.*, 2016, **28**, 2573–2580.
25 D. J. Lun, G. I. N. Waterhouse and S. G. Telfer, *J. Am. Chem. Soc.*, 2011, **133**, 5806–5809.
26 Y. C. Lien and W. W. Nawar, *J. Food Sci.*, 1974, **39**, 911–913.
27 Y. C. Lien and W. W. Nawar, *J. Food Sci.*, 1974, **39**, 914–916.

 This journal is © The Royal Society of Chemistry 2020